COMPUTATIONAL PHOTOANALYSIS SOFTWARE FOR MARTIAN SOIL GRANULOMETRY.

Siyuan Zhao[1], Yutong Shi[1], Suniti Karunatillake[2], and Long Xiao[1], [1]Planetary Science Institute, School of Earth Sciences, China University of Geosciences, Wuhan, China (longxiao@cug.edu.cn), [2]Louisiana State University, E235 Howe-Russell, Baton Rouge, LA 70803, United States.

Introduction: Photoanalytical segmentation of individual soil grains and granulometry in high-resolution surface images are key in understanding geologic processes of planetary bodies before sample return to Earth. Previous studies of Mars soil granulometry have majorly relied on manual identification [1,2] or image processing programs originated from other fields, such as ImageJ [3,4,5]. Those methods have obtained optimal outcomes in certain images but still require heavy labor to editing the segmentation or fine-tuning the parameters, and to classifying the granulometry results. Other algorithmic segmentation methods that are commonly used in terrestrial cases, such as MATLAB-based BASEGRAIN for fluvial gravel beds [6], or commercial software WipFrag and Fragscan for rock fragments, are neither proved to be most effective in planetary soil analyses. Newly developed machine learning based methods, such as the trainable WEKA segmentation tools in ImageJ [7] and the supervised classification tools in ENVI have shown advantages handling complex cases, yet their commonly adopted threshold segmentation method leads to effective distinguishing of areas rather than outlining grains with close boundaries, and the requirement of training datasets creates increased workloads.

Here we present a Mathematica-based semi-automated image segmenting software tool that allows faster segmentation and granulometry analysis of planetary (soil) images based on the algorithm of Karunatillake et al. (2013, 2014), with a graphical user interface (GUI) to increase the software accessibility. So far, our software has been adapted to several Martian in-situ observation images including the Mars Hand Lens Imager (MAHLI) at Gale Crater and Microscopic Imager (MI) and is aimed to expand its application to images of the Moon and the asteroids.

Method: Our software provides segmenting and granulometry measurement of Martian soil images through steps below, with several manual guide points: (1) Image imported: all common raster images are supported, as well as the IMG formatted MAHLI and MI images. While the MI image possesses a constant pixel size of 31 µm/pixel [8], for MAHLI images with various focal lengths, a focus motor count is required to calculate pixel size. The imported images are processed with gamma correction, contrast adjustment, background sharpen, and are visually decided whether there is a distinct foreground before going to the second step: (2) Image segmented: two independent modules are designed for segmenting the foreground and background with separate parameters, the coarser-grained foreground was masked before the finer-grained background is segmented. The GUI allows dynamic visualization of how the segmenting result changes with each parameter, facilitating the setting of parameters. Algorithmic details of segmentation are depicted in our prior works [9,10]. (3) Granulometry: in this step, the grain size is calculated from the focal length and Wentworth classification of detected grains is established [11], highlighting the dominant class of grain size. The probability density and cumulative distribution of grain size can also be plotted. Finally, the parameters used and granulometry results as well as other options in the “Display” are supported to export.

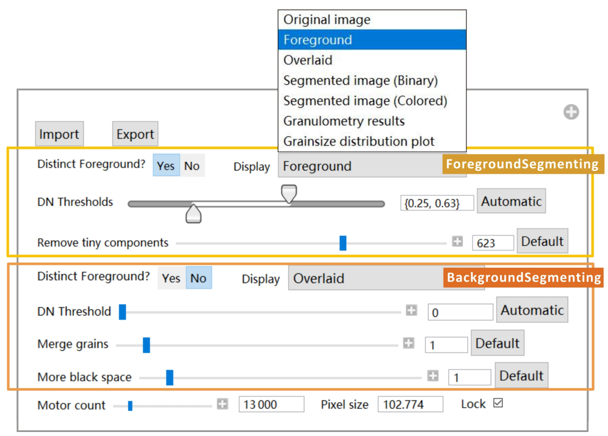

Fig. 1: GUI of our computational photoanalysis software, which allow a two-step segmentation of image foreground and background.

Result and discussion:

To check the performance of our software, we qualitatively tested our software with 57 MAHLI and MI images with or without foreground, with comparison to BASEGRAIN, ImageJ Trainable Weka Segmentation tools, ENVI Classification tools and Feature Extraction tools. Our software has not only the fastest speed but also the best accuracy.

The region-based segmentation algorithm is adopted both in our software and in BASEGRAIN. Compared to BASEGRAIN, our software shows better results in reducing the influence of shadow and distinguishing higher orders of size difference across grains in a sample [9], even without the manual merging and graindeleting features of BASEGRAIN. Clustering based (i.e. ENVI unsupervised classification tools) and supervised segmentation methods (i.e. ENVI supervised classification tools and ImageJ Trainable Weka Segmentation tool) segment image according to pixel's color and pixels with similar colors are usually classified into one category. Thus, these methods are insufficient to distinguish adjacent grains with similar colors which are commonly observed on the red-hued Mars. What's more, although the foreground normally has higher brightness, the various brightness value of the background would add difficulties to foreground extracting. Similar methods would conduct sufficient segmentation on terrestrial images with sediments of complex composition and various colors.

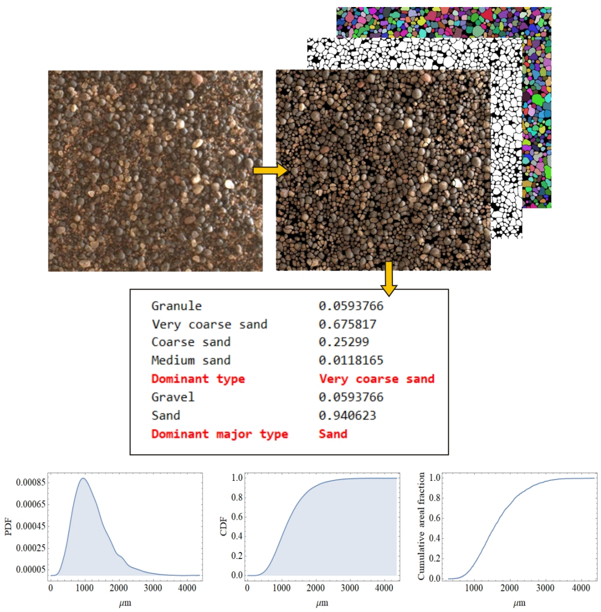

Fig. 2: Major inputs and outputs of our photoanalysis software, including the segmented images and granulometry results.

Edge detection based method is adopted in ENVI Classification tools and Feature Extraction tools, however, the performance of edge detection is unsatisfactory, and some distinct foreground edges are not extracted. ENVI Feature Extraction tools use variational DN values to represent the segments in the segmentation image. However, in our software, boundaries of 1- 2 pixels' wide delineating the grain boundary are considered as unclassified areas in grain size calculation, leading to granulometry results smaller than actual grain sizes, especially for the finer grains.

Aside from the low inter-grain brightness or color contrast as discussed above, there are other factors that would affect the accuracy of grain segmenting, such as the image resolution, the camera angle, and the influence of shadows. Shadows usually coexist with foreground rocks, covering part of the rock surface and the background. The shadowed part of rock, with surface brightness even lower than some pixels in the background, is found difficult to be identified as foreground, leading to segmenting errors. For the shadowed background, some small grains with low brightness would be identified as black spaces between grains, leading to more unclassified areas.

Conclusion and future work: Aiming to serve the needs of Martian sediments photoanalysis, we developed a semi-automated image segmenting software that could conduct fast grain segmenting and granulometry measurement of the MAHLI and MI images, and provide results comparable to other commonly used methods. In future work, a particle morphometry measuring function will be added so that statistics of grain roundness, sphericity, and angularity could be obtained. High-resolution images from the moon and the asteroids will also be used in software testing to expand the range of its applicability to other planetary bodies. We will also consider its application on terrestrial cases, such as images of terrestrial sediments or petrological thin sections, which will need further improvement of the software concerning the increased compositional and optical complexity of terrestrial grains.

Acknowledgments: This study was supported by the Pre-research Project on Civil Aerospace Technologies of CNSA (D020101). All original MAHLI and MI data can be obtained from the NASA's Planetary Data System (http://pds.nasa.gov/).

References: [1] McGlynn et al., (2011) *JGR, 116,* E00F22. [2] Karunatillake et al., (2010) *JGR, 115,* E00F04. [3] Cousin et al., (2017) *JGR, 122,* 2144–2162. [4] Rivera-Hernández et al., (2019) *Icarus, 321,* 82- 98. [5] Weitz et al., (2018) *GRL, 45,* 10.1029/2018GL078972. [6] Detert and Weitbrecht, (2012) *River Flow 2012, ISBN 978-0-415-62129-8,* 595-600. [7] Arganda-Carreras et al., (2017) *Bioinformatics, 33,* 2424–2426. [8] Herkenhoff et al. (2003) *JGR, 108*: 8065. [9] Karunatillake et al., (2014) *Icarus, 229,* 400- 407. [10] Karunatillake et al., (2014) *Icarus, 229,* 408- 417. [11] Wentworth (1922) *Journal of Geology, 30,* 377- 392.